Journal of Power Sources 196 (2011) 3544–3547

Contents lists available at ScienceDirect

Journal of Power Sources

journal homepage: www.elsevier.com/locate/jpowsour

Short communication

Nano-structured cathodes based on $La_{0.6}Sr_{0.4}Co_{0.2}Fe_{0.8}O_{3-\delta}$ for solid oxide fuel cells

Ju Hee Kim[a], Young Min Park[b], HaeKyoung Kim[a,*]

[a] School of Materials Science & Engineering, Yeungnam University, 214-1 Deadong, Gyeongsan, Gyeongbuk 712-749, Republic of Korea
[b] Fuel Cell Project, Research Institute of Industrial Science and Technology, Pohang 790-330, Republic of Korea

ARTICLE INFO

Article history:
Received 6 October 2010
Received in revised form
27 November 2010
Accepted 2 December 2010
Available online 21 December 2010

Keywords:
Solid oxide fuel cell
Nano dispersant
Anode supported
Mixed ionic electronic conductor
Perovskite

ABSTRACT

Lanthanum-based iron- and cobalt-containing perovskite is a promising cathode material because of its electrocatalytic activity at a relatively low operating temperature in solid oxide fuel cells (SOFCs), i.e., 700–800 °C. To enhance the electrocatalytic reduction of oxidants on $La_{0.6}Sr_{0.4}Co_{0.2}Fe_{0.8}O_{3-\delta}$ (LSCF), nanocrystalline LSCF materials are successfully fabricated using a complexing method with chelants and inorganic nano dispersants. When inorganic dispersants are added to the synthesis process, the surface area of the LSCF powder increases from 18 to 88 $m^2\,g^{-1}$, which results in higher electrocatalytic activity of the cathode. The performance of a unit cell of a SOFC with nanocrystalline LSCF powders synthesized with nano dispersants is increased by 60%, from 0.7 to 1.2 $W\,cm^{-2}$.

1. Introduction

Solid oxide fuel cells (SOFCs) are considered to be promising candidates for the future of energy generation systems for power plants and distributed power. For a state-of-the-art anode-supported SOFC operating at 800 °C, the performance of a conventional $La_{1-x}Sr_xMnO_{3-\delta}$ (LSM)-based cathode is not satisfactory due to sluggish oxygen reduction reaction (ORR) kinetics that cause a low current drawing capacity of the cell [1,2]. Moreover, most of the electrochemical reactions in LSM-based cathodes using pure electronic conducting materials are restricted to the triple-phase boundary of the electronic conducting sites, the ionic conducting sites and the gaseous oxygen. Hence, considerable efforts are being made to develop a new class of perovskite-based cathode materials for SOFCs that have mixed ionic and electronic conductivity with a high electrocatalytic activity for oxygen reduction at a relatively lower operating temperature (700–800 °C) [1–11]. Amongst these, lanthanum-based iron- and cobalt-containing perovskites (LSCF) are good candidates for SOFC cathode materials, because of their high electronic and oxygen ion conductivity as well as electro-catalytic activity. With a Gd-doped ceria (GDC)-based interlayer, perovskite-based compounds with the general formula $La_{0.6}Sr_{0.4}Co_{0.2}Fe_{0.8}O_{3-\delta}$ have been reported to be very effective for IT-SOFC (700–800 °C) applications. This is because of the high catalytic activity of LSCF and suppression of the formation of resistive phases such as strontium zirconate due to the GDC diffusion blocking layer [5,6,10–14].

The electrochemical performance of anode-supported SOFCs with a LSCF-type cathode can also be varied by processing and by the micro-structural parameters of the cathode materials [5,14]. A small particle-size and a high surface area of nanocrystalline materials are favoured for the cathode electrode of SOFCs [15,16], which results in enhanced electrocatalytic reduction of oxidant along with higher catalytic activity [17–20]. The nanocrystalline cathodes can be easily sintered and the extent of sinterability of these powders can be controlled by the amount of the organic compounds added during the preparation of the thick film paste for screen printing. Nevertheless, the high temperatures required for phase formation of IT-SOFC cathode materials hinder the formation of nanostructures [20–22]. In this study, LSCF-based nanocrystalline powders are prepared by a complexing method with ethylene diamine tetra-acetic acid (EDTA) and citric acid as chelants to reduce the temperature required for phase formation. Inorganic nano dispersants are used to control the distribution and size of nanocrystalline LSCF. The LSCF-based cathode powders synthesized with inorganic nano dispersants are characterized for structural, thermal and electrical properties, and then compared with a powder that is synthesized without inorganic nano dispersants. The electrochemical performance of the Ni-YSZ support/Ni-YSZ anode functional layer/YSZ electrolyte/GDC interlayer anode-supported cells is evaluated with synthesized cathode materials to study the effects of inorganic nano dispersants.

* Corresponding author. Tel.: +82 53 810 2536; fax: +82 53 810 4628.
E-mail address: hkkim@ynu.ac.kr (H. Kim).

0378-7753/$ – see front matter © 2010 Elsevier B.V. All rights reserved.
doi:10.1016/j.jpowsour.2010.12.029

2. Experimental procedure

Lanthanum nitrate, strontium nitrate, cobalt nitrate and ferric nitrate, all in analytical grades, were used as metal sources. EDTA powder and crystallized citric acid served as the raw materials for chelation and both have purities greater than 99.5%. 7.79 g (0.018 mol) of lanthanum nitrate ($La(NO_3)_3{\cdot}6H_2O$), 2.53 g (0.012 mol) of strontium nitrate ($Sr(NO_3)_2$), 1.74 g (0.006 mol) of cobalt nitrate ($Co(NO_3)_2{\cdot}6H_2O$), and 9.7 g (0.024 mol) of ferric nitrate ($Fe(NO_3)_3{\cdot}9H_2O$) were dissolved in 100 ml of deionized water to prepare a homogeneous metal nitrate solution. Solid citric acid of 11.47 g (0.06 mol) was added to the mixed metal nitrate solution. 8.77 g (0.03 mol) of EDTA powder was introduced and the solution was heated in a water bath at 70 °C. After obtaining a clear solution, HI BLACK170 (HB170, low colour furnace carbon black) with a surface area of 23 $m^2\,g^{-1}$ and a particle size of 58 nm was added as an inorganic nano dispersant. Three types of batch were prepared, namely: HB-0 (without HB170), HB-3 (with 3 g of HB170), and HB-5 (with 5 g of HB170). The mixture was reheated to evaporate the water until the magnetic bar ceased rotating. The remaining mixture was dried at 80–120 °C in a vacuum oven overnight to remove residual water. The dried powders were crushed and calcined to form a perovskite phase and removing the organic compounds and inorganic nano dispersants. The calcined powders were characterized by means of X-ray diffraction and scanning electron microscopy (SEM) to observe the phase and the morphologies. Thermogravimetric analysis (TGA) was carried out from room temperature to 1000 °C in air at a heating rate of 3 °C min^{-1} using a Shimadzu TA-50 Thermal Analyzer to investigate the thermal behaviour. The specific surface-area (SSA) of the powder was calculated by the BET method from nitrogen adsorption isotherms. To evaluate the fuel cell performance, the synthesized powders were mixed with ESL449 from ESL. The Ni-YSZ/YSZ/GDC anode-supported cells were cut into 1-in. diameter circles from a 25 cm × 25 cm plate prepared by a co-fired method. The cathode paste was printed on the Ni-YSZ/YSZ/GDC anode-supported cell and sintered at 1000 °C for 4 h. The cell area was 0.785 cm^2. The fuel cell performances were tested with a 300 $cm^3\,min^{-1}$ of 97% H_2–3% H_2O and 1000 $cm^3\,min^{-1}$ of air.

3. Results and discussion

The thermal analysis curves of the mixtures after drying at 80–120 °C are presented in Fig. 1. Significant weight losses in the HB-0 batch were observed at ~175 and 300 °C due to the decomposition of organic compounds, citric acid, and EDTA. The batches of HB-3 and HB-5 experience additional weight losses at 380–450 °C due to decomposition of the HB170. The organic chelants and nano dispersants during the synthesis process of the nanacrystalline LSCF cathode are decomposed below 600 °C. From 550 °C, the weight loss is not observed and the heat flows for phase formation are characterized. The perovskite peak of LSCF in all the batches appears from 600 °C in the XRD spectra, as shown in Fig. 2, which is at a relatively lower temperature compared with combustion methods or other powder processes [20–22].

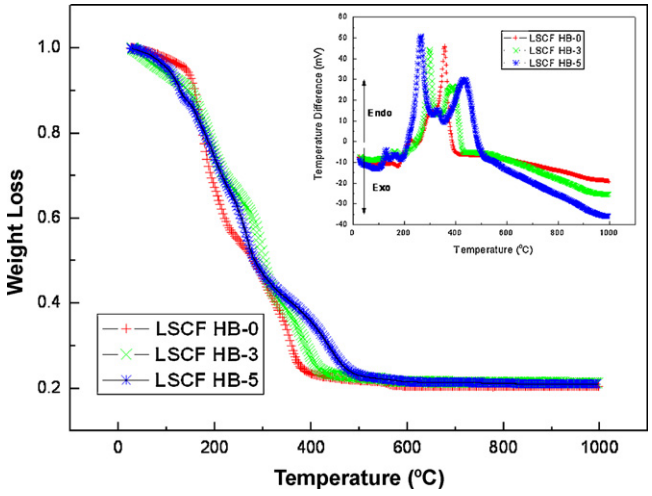

Fig. 1. TGA measurements of LSCF powders.

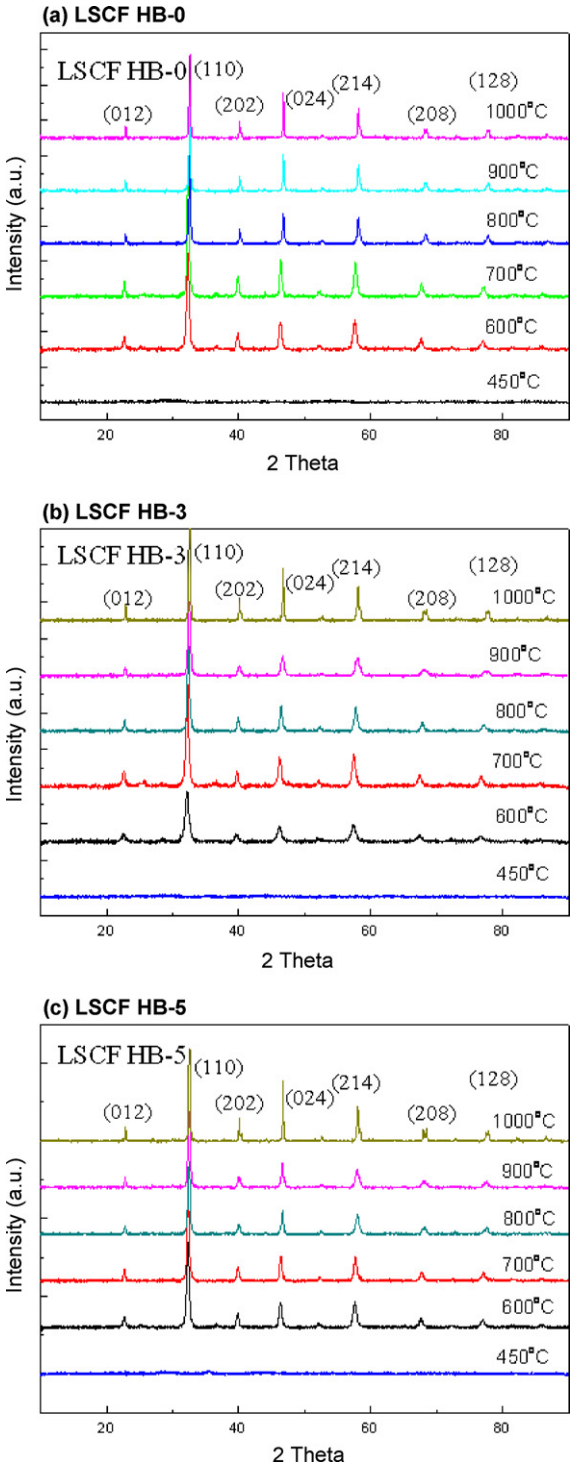

Fig. 2. XRD patterns of LSCF powders as function of temperature.

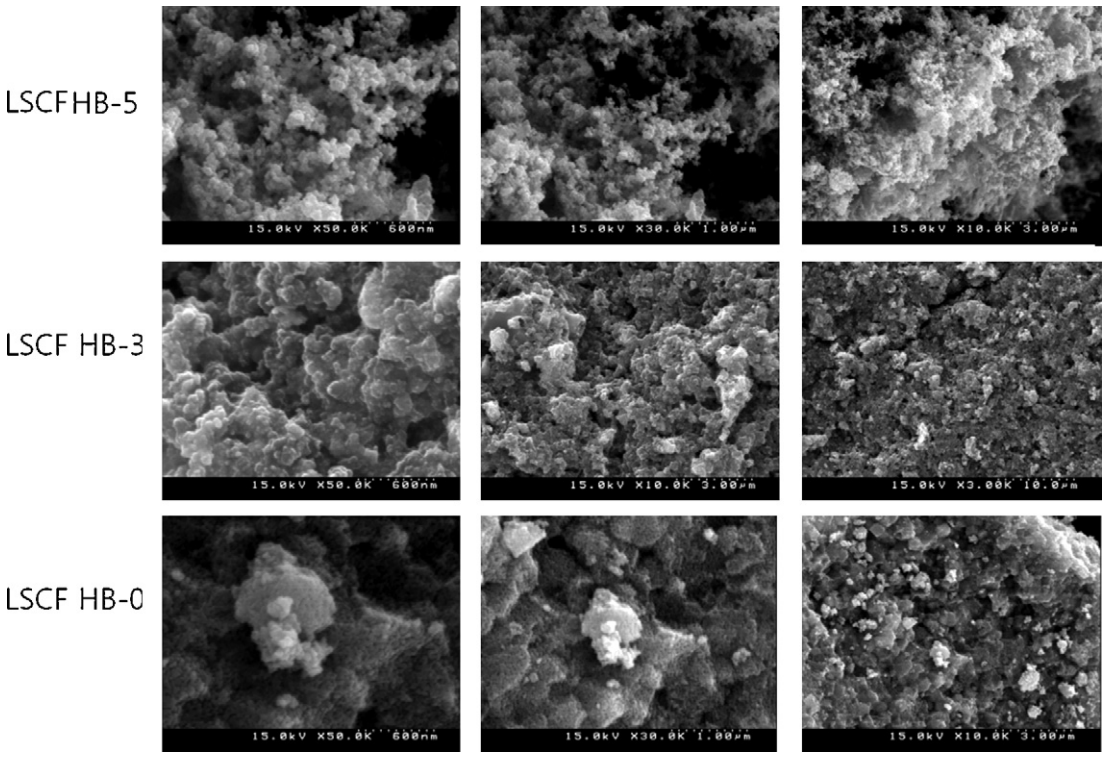

Fig. 3. SEM images of LSCFs after calcination at 700 °C for 5 h.

The size of the calcined powder at 700 °C of HB-0 was ~60 nm and agglomerated morphologies are easily observed, as shown in Fig. 3. With the addition of nano dispersant in HB-3 and HB-5, the particles are well dispersed and agglomerated clusters are rarely observed. The surface area characterized by BET measurement shows an increase with addition of inorganic nano dispersants from 18 $m^2\ g^{-1}$ of HB-0 to 55 $m^2\ g^{-1}$ of HB-3 and 88 $m^2\ g^{-1}$ of HB-5. The BET results are in accordance with the morphologies from SEM images. In summary, the nano dispersant is very effective for preventing agglomeration.

To investigate fuel cell performance, LSCF pastes were prepared with organic compounds, ESL 449, and printed on the Ni-YSZ/YSZ/GDC anode-supported cell. It has been reported that the sintering temperature for LSCF-based cathodes should be optimized to obtain the best cell performance [23]. In this study, however to investigate the effects of the nano dispersants, the cathodes were sintered at 1000 °C and the electrochemical performances were characterized as shown in Fig. 4. At 780 °C, the maximum power density of the SOFC cells with HB-0, HB-3 and HB-5 is 0.71, 1.05, and 1.16 W cm^{-2}, respectively. With the addition of nano dispersant in HB-3, the fuel cell performance increases

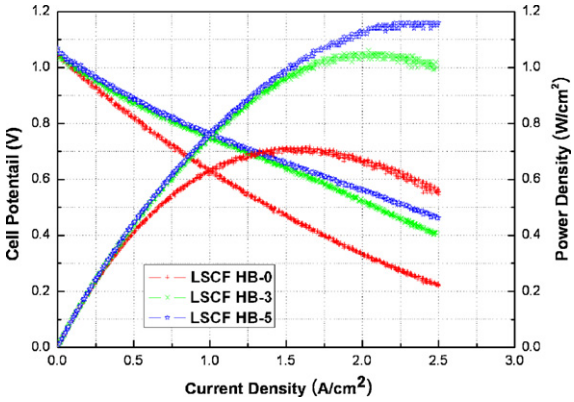

Fig. 4. Fuel cell performance of SOFCs with synthesized cathode materials at 780 °C.

from 0.71 to 1.05 W cm^{-2}. The increase of performance is considered to be due primarily to the higher electrocatalytic activity of the cathode synthesized with nano dispersants. The microstructures of the studied cathodes were analyzed after electrochemical charac-

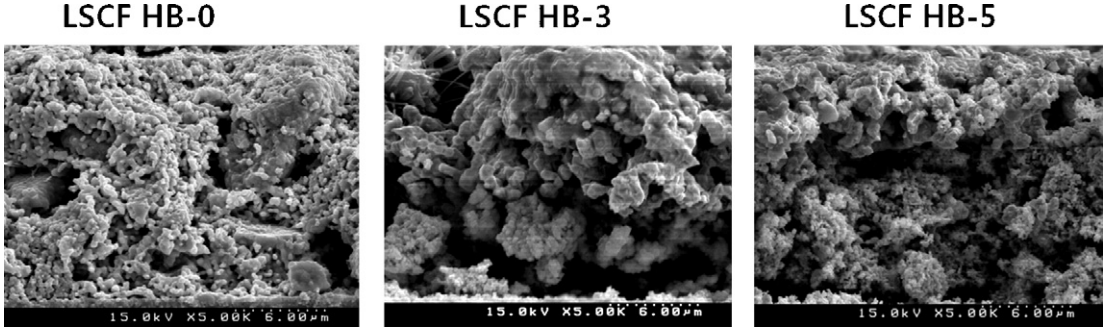

Fig. 5. Microstructures of cathodes with synthesized LSCF powders.

terization and are shown in Fig. 5. The cross-sectional images of the cells with cathodes from HB-3 and HB-5 display a much longer TPB length with smaller size particles than that from HB-0. The longer TPB length of the LSCF cathode synthesized with the nano dispersant results in superior electrochemical performance.

To compare the polarization of cells, the area-specific resistances (ASRs) of each cell were calculated from the linear portion of the current–voltage characteristics corresponding to a cell voltage from 1.0 to 0.7 V [24]. The total ASR value of the cell consists of the ohmic resistance from the electrolyte, electrodes, and corresponding interfaces, and polarization resistances at the electrode|electrolyte interface. The ASRs for cells with HB-5 and HB-3 cathodes are much lower (0.26 and 0.27 $\Omega\,cm^2$) than that with HB-0 (0.42 $\Omega\,cm^2$). A cathode with an increased TPB and electrocatalytic activity due to extensive surface areas results in a lower total ASR and a higher fuel cell performance. In an anode-supported single-cell with a Gd-doped ceria interlayer, the $La_{0.6}Sr_{0.4}Co_{0.2}Fe_{0.8}O_{3-\delta}$ cathode synthesized with the addition of nano dispersants yields a superior electrochemical performance. This study reconfirms that the microstructure of cathode materials should be considered as an important parameter, in addition to the composition. To obtain higher fuel cell performance with a lower ASR, more studies are required on the sintering temperature and long term stability to optimize the cathode microstructure.

4. Conclusions

Nanocrystalline cathode materials based on $La_{0.6}Sr_{0.4}Co_{0.2}Fe_{0.8}O_{3-\delta}$ have been successfully synthesized by a complexing method with inorganic nano dispersants and chelants. The phase formation for perovskite starts at 600 °C, which is a relatively low temperature. The surface area of the LSCF cathode materials without nano dispersants is 11 $m^2\,g^{-1}$ and the surface area increases to 55–88 $m^2\,g^{-1}$ when nano dipersants and nano-sized-carbon black, are added. The nano dispersant is very beneficial for controlling the particle size of the LSCF. Calcined LSCF powders at 700 °C from HB-0, HB-3, and HB-5 are used for cathode pastes, which are screen-printed on an anode supported cell, which has a configuration of Ni-YSZ support/Ni-YSZ anode functional layer/YSZ electrolyte/GDC interlayer, and sintered at 1000 °C for 4 h. The electrochemical performances of cathodes from the HB-5 and HB-3 batches are 1.16 and 1.05 $W\,cm^{-2}$, respectively, of the maximum power density at 780 °C and much higher than that from HB-0, 0.71 $W\,cm^{-2}$. The ASRs are calculated from the linear portion of the current–voltage characteristics and those of the HB-5 and HB-3 cathodes are 0.26 and 0.27 $\Omega\,cm^2$, respectively, and much lower than that of HB-0 (0.42 $\Omega\,cm^2$). Cathodes synthesized with inorganic nano dispersants have a higher active surface area, which results in higher electrochemical performances because of the higher electrocatalytic surface area and the unique morphologies.

Acknowledgement

This work was supported by Yeungnam University research grants in 2008.

References

[1] S.P. Jiang, Solid State Ionics 146 (2002) 1–22.
[2] M.J. Jørgensen, M. Mogensen, J. Electrochem. Soc. 148 (2001) A433–A442.
[3] V. Dusastre, J.A. Kilner, Solid State Ionics 126 (1999) 163–174.
[4] D. Kušščer, J. Holc, S. Hrovat, D. Kolar, J. Eur. Ceram. Soc. 21 (2001) 1817–1820.
[5] A. Mai, V.A.C. Haanappel, S. Uhlenbruck, F. Tietz, D. Stöver, Solid State Ionics 176 (2005) 1341–1350.
[6] A. Mai, V.A.C. Haanappel, S. Uhlenbruck, F. Tietz, D. Stöver, Solid State Ionics 177 (2006) 2103–2107.
[7] Y. Teraoka, H.M. Zhang, K. Okamoto, N. Yamazoe, Mater. Res. Bull. 23 (1988) 51–58.
[8] J. Fleig, J. Power Sources 105 (2002) 228–238.
[9] S.B. Adler, J.A. Lane, B.C.H. Steele, J. Electrochem. Soc. 143 (1996) 3554–3564.
[10] J.A. Kilner, R.A. De Souza, I.C. Fullarton, Solid State Ionics 86–88 (1996) 703–709.
[11] J. Fleig, Annu. Rev. Mater. Res. 33 (2003) 361–382.
[12] V.V. Srdic, R.P. Omorjan, J. Seidel, Mater. Sci. Eng. B 116 (2005) 119–124.
[13] E.P. Murray, M.J. Sever, S.A. Barnett, Solid State Ionics 148 (2002) 27–34.
[14] V.A.C. Haanappel, J. Mertens, D. Rutenbeck, C. Tropartz, W. Herzhof, D. Sebold, F. Tietz, J. Power Sources 141 (2005) 216.
[15] N. Gunasekaran, S. Saddawi, J.J. Carberry, J. Catal. 159 (1996) 107–111.
[16] Y. Liu, H.T. Zheng, J.R. Liu, T. Zhang, Chem. Eng. J. 89 (2002) 213–221.
[17] A. Dutta, J. Mukhopadhyay, R.N. Basu, J. Eur. Ceram. Soc. 29 (2009) 2003–2011.
[18] S. Shukla, S. Seal, R. Vij, S. Bandyopadhyay, Nano Lett. 3 (2003) 397–401.
[19] Q.S. Zhu, B.A. Fan, Solid State Ionics 176 (2005) 889–894.
[20] M.G. Bellino, D.G. Lamas, N.E.W. de Reca, Adv. Funct. Mater. 16 (2006) 107–113.
[21] W. Zhou, Z.P. Shao, W.Q. Jin, J. Alloys Compd. 426 (2006) 368–374.
[22] L. Baqué, A. Caneiro, M.S. Moreno, A. Serquis, Electrochem. Commun. 10 (2008) 1905–1908.
[23] F. Tietz, V.A.C. Haanappel, A. Mai, J. Mertens, D Stöver, J. Power Sources 156 (2006) 20–22.
[24] J.W. Kim, A.V. Virkar, K.Z. Fung, K. Mehta, S.C. Singhal, J. Electrochem. Soc. 146 (1) (1999) 69–78.